Machine-learning classification suggests that many alphaproteobacterial prophages may instead be gene transfer agents

Roman Kogay[1], Taylor B. Neely[1,2], Daniel P. Birnbaum[1,3], Camille R. Hankel[1,4], Migun Shakya[1,5], and Olga Zhaxybayeva[1,6,*]

[1] Department of Biological Sciences, Dartmouth College, Hanover, NH, USA

[2] Present address: Amazon.com Inc., Seattle, WA, USA

[3] Present address: School of Engineering and Applied Sciences, Harvard University, Cambridge, MA, USA

[4] Present address: Department of Earth and Planetary Sciences, Harvard University, Cambridge, MA, USA

[5] Present address: Bioscience Division, Los Alamos National Laboratory, Los Alamos, NM, USA

[6] Department of Computer Science, Dartmouth College, Hanover, NH, USA

* Author for Correspondence: Olga Zhaxybayeva, Department of Biological Sciences, Dartmouth College, Hanover, NH, USA, Tel: 603-646-8616, E-mail: olga.zhaxybayeva@dartmouth.edu

Data deposition

Sequence alignments and phylogenetic trees are available in a **FigShare** repository at DOI 10.6084/m9.figshare.8796419. The Python source code of the described classifier and additional scripts used in the analyses are available via a **GitHub** repository at https://github.com/ecg-lab/GTA-Hunter-v1

Abstract

Many of the sequenced bacterial and archaeal genomes encode regions of viral provenance. Yet, not all of these regions encode *bona fide* viruses. Gene transfer agents (GTAs) are thought to be former viruses that are now maintained in genomes of some bacteria and archaea and are hypothesized to enable exchange of DNA within bacterial populations. In Alphaproteobacteria, genes homologous to the 'head-tail' gene cluster that encodes structural components of the *Rhodobacter capsulatus* GTA (RcGTA) are found in many taxa, even if they are only distantly related to *Rhodobacter capsulatus*. Yet, in most genomes available in GenBank RcGTA-like genes have annotations of typical viral proteins, and therefore are not easily distinguished from their viral homologs without additional analyses. Here, we report a 'support vector machine' classifier that quickly and accurately distinguishes RcGTA-like genes from their viral homologs by capturing the differences in the amino acid composition of the encoded proteins. Our open-source classifier is implemented in Python and can be used to scan homologs of the RcGTA genes in newly sequenced genomes. The classifier can also be trained to identify other types of GTAs, or even to detect other elements of viral ancestry. Using the classifier trained on a manually curated set of homologous viruses and GTAs, we detected RcGTA-like 'head-tail' gene clusters in 57.5% of the 1,423 examined alphaproteobacterial genomes. We also demonstrated that more than half of the *in silico* prophage predictions are instead likely to be GTAs, suggesting that in many alphaproteobacterial genomes the RcGTA-like elements remain unrecognized.

Keywords

Virus exaptation, GTA, *Rhodobacter capsulatus*, support vector machine, binary classification, carbon depletion

Introduction

Viruses that infect bacteria (phages) are extremely abundant in biosphere (Keen 2015). Some of the phages integrate their genomes into bacterial chromosomes as part of their infection cycle and survival strategy. Such integrated regions, known as prophages, are very commonly observed in sequenced bacterial genomes. For example, Touchon et al. (2016) report that 46% of the examined bacterial genomes contain at least one prophage. Yet, not all of the prophage-like regions represent *bona fide* viral genomes (Koonin and Krupovic 2018). One such exception is a Gene Transfer Agent, or GTA for short (reviewed most recently in Lang et al. (2017) and Grull et al. (2018)). Many of genes that encode GTAs have significant sequence similarity to phage genes, but the produced tailed phage-like particles generally package pieces of the host genome unrelated to the "GTA genome" (Hynes et al. 2012; Tomasch et al. 2018). Moreover, the particles are too small to package complete GTA genome (Lang et al. 2017). Hence, GTAs are different from lysogenic viruses, as they do not use the produced phage-like particles for the purpose of their propagation.

Currently, five genetically unrelated GTAs are known to exist in Bacteria and Archaea (Lang et al. 2017). The best studied GTA is produced by the alphaproteobacterium *Rhodobacter capsulatus* and is referred hereafter as the RcGTA. Since RcGTA's discovery 45 years ago (Marrs 1974), the genes for the related, or RcGTA-like, elements have been found in many of the alphaproteobacterial genomes (Shakya et al. 2017). For a number of *Rhodobacterales* isolates that carry RcGTA-like genes, there is an experimental evidence of GTA particle production (Fu et al. 2010; Nagao et al. 2015; Tomasch et al. 2018). Seventeen of the genes of the RcGTA "genome" are found clustered in one locus and encode proteins that are involved in DNA packaging and head-tail morphogenesis (**Figure 1** and **Supplementary Table S1**). This locus is referred to as a 'head-tail cluster'. The remaining seven genes of the RcGTA genome are distributed across four loci and are involved in maturation, release and regulation of RcGTA production (Hynes et al. 2016). Since the head-tail cluster resembles a typical phage genome with genes organized in modules similar to those of a λ phage genome (Lang et al. 2017), and since many of its

genes have homologs in *bona fide* viruses and conserved phage gene families (Shakya et al. 2017), the cluster is usually designated as a prophage by algorithms designed to detect prophage regions in a genome (Shakya et al. 2017). The RcGTA's classification as a prophage raises a possibility that some of the '*in silico*'-predicted prophages may instead represent genomic regions encoding RcGTA-like elements.

Currently, to distinguish RcGTA-like genes from the truly viral homologs one needs to examine evolutionary histories of the RcGTA-like and viral homologs and to compare gene content of a putative RcGTA-like element to the RcGTA "genome". These analyses can be laborious and often require subjective decision making in interpretations of phylogenetic trees. An automated method that could quickly scan thousands of genomes is needed. Notably, the RcGTA-like genes and their viral homologs have different amino acid composition (**Figure 1** and **Supplementary Figure S1**). Due to the purifying selection acting on the RcGTA-like genes at least in the *Rhodobacterales* order (Lang et al. 2012) and of their overall significantly lower substitution rates when compared to viruses (Shakya et al. 2017), we hypothesize that the distinct amino acid composition of the RcGTA-like genes is preserved across large evolutionary distances, and therefore the RcGTA-like genes can be distinguished from their *bona fide* viral homologs by their amino acid composition.

Support vector machine (SVM) is a machine learning algorithm that can quickly and accurately separate data into two classes from the differences in specific features within each class (Cortes and Vapnik 1995). The SVM-based classifications have been successfully used to delineate protein families (e.g., DNA binding proteins (Bhardwaj et al. 2005) and G-protein coupled receptors (Karchin et al. 2002)), to distinguish plastid and eukaryotic host genes (Kaundal et al. 2013), and to predict influenza host from DNA and amino acid oligomers found in the sequences of the flu virus (Xu et al. 2017). During the training step, the SVM constructs a hyperplane that best separates the two classes. During the classification step, data points that fall on one side of the hyperplane are assigned to one class, while those on the other side are assigned to the other class. In our case, the two classes of elements in need of

separation are phages and GTAs, while their distinguishing features are several metrics that capture the amino acid composition of the encoding genes.

In this study, we developed, implemented, and cross-validated an SVM classifier that distinguishes RcGTA-like head-tail cluster genes from their phage homologs with high accuracy. We then applied the classifier to 1,423 alphaproteobacterial genomes to examine prevalence of putative RcGTA-like elements in this diverse taxonomic group and to assess how many of the RcGTA-like elements are mistaken for prophages in the *in silico* predictions.

Materials and Methods

The Support Vector Machine (SVM) classifier and its implementation

Let's denote as u a homolog of an RcGTA-like gene g that needs to be assigned to a class y, "GTA" ($y = -1$) or "virus" ($y = 1$). The assignment is carried out using a weighted soft-margin SVM classifier, which is trained on a dataset of m sequences $T^g = \{T_1^g, \dots, T_m^g\}$ that are homologous to u (see **"SVM training data"** section below). The basis of the classification is the *n*-dimensional vector of features $\boldsymbol{x}$ associated with sequences u and T_i^g (see **"Generation of sequence features"** section below). Each sequence T_i^g is known to belong to a class y_i.

Using the training dataset T^g, we identify hyperplane that separates two classes as an optimal solution to the objective function:

$$min\left(\frac{1}{2}||\boldsymbol{w}||^2 + \boldsymbol{C}\sum_{i=1}^{m}\xi_i\right) \text{ (eq. 1)}$$

subject to:

$$\forall_i\colon\ y_i(\boldsymbol{w}\boldsymbol{x_i} + b) \geq 1 - \xi_i, where\ \xi_i \geq 0, i = 1, \dots, m \text{ (eq. 2)}$$

where $\boldsymbol{w}$ and b define the hyperplane $f(\boldsymbol{x}) = \boldsymbol{w}\boldsymbol{x_i} + b$ that divides the two classes, ξ_i is the slack variable that allows some training data points not to meet the separation requirement, and $\boldsymbol{C}$ is a regularization parameter, which is represented as an $m \times m$ diagonal matrix. The $\boldsymbol{C}$ matrix determines how lenient the soft-margin SVM is in allowing for genes to be misclassified: larger values "harden" the margin, while smaller values "soften" the margin by allowing more classification errors. The product $\boldsymbol{C}\xi$ represents the cost of misclassification. The most suitable values for the $\boldsymbol{C}$ matrix were determined empirically during cross-validation, as described in the **"Model training, cross validation, and assessment"** section below.

To solve equation 1, we represented this minimization problem in the Lagrangian dual form $L(\alpha)$:

$$\max_{\alpha_i} \quad L(\alpha) = \sum_{i=1}^{m} \alpha_i - \frac{1}{2}\sum_{i=1}^{m}\sum_{i=j}^{m} \alpha_i \alpha_j y_i y_j K(\boldsymbol{x}_i \boldsymbol{x}_j)\ \ (eq. 3)$$

subject to:

$$\forall_i\colon \sum_{i=1}^{m} \alpha_i y_i = 0\ and\ 0 \leq \alpha_i \leq C, \qquad i = 1, \dots, m$$

where K represents a kernel function. The minimization problem was solved using the convex optimization (CVXOPT) quadratic programming solver (Andersen et al. 2012). The pseudocode of the algorithm for the weighted soft-margin SVM classifier training and prediction is shown in **Figure 2**.

SVM training data

To train the classifier, sets of "true viruses" (class $y = 1$) and "true GTAs" (class $y = -1$) were constructed separately for each RcGTA-like gene g. To identify the representatives of "true viruses", amino acid sequences of 17 genes from the RcGTA head-tail cluster were used as queries in BLASTP (E-

132 value < 0.001; query and subject overlap by at least 60% of their length) and PSI-BLASTP searches (E-
133 value < 0.001; query and subject overlap by at least 40% of their length; maximum of six iterations) of
134 the viral RefSeq database release 90 (last accessed in November 2018; accession numbers of the viral
135 entries are provided in **Supplementary Table S2**). BLASTP and PSI-BLAST executables were from the
136 BLAST v. 2.6.0+ package (Altschul et al. 1997) . The obtained homologs are listed in **Supplementary**
137 **Table S3**. Due to few or no viral homologs for some of the queries, the final training sets T^g were limited
138 to 11 out of 17 RcGTA-like head-tail cluster genes (*g2, g3, g4, g5, g6, g8, g9, g12, g13, g14, g15*; see
139 **Supplementary Table S1** for functional annotations of these genes).

140 To identify the representatives of "true GTAs", amino acid sequences of 17 genes from the
141 RcGTA head-tail cluster (Lang et al., 2017) were used as queries in BLASTP (E-value < 0.001; query and
142 subject overlap by at least 60% of their length) and PSI-BLAST searches (E-value < 0.001; query and
143 subject overlap by at least 40% of their length; maximum of six iterations) of the 235 complete
144 alphaprotebacterial genomes that were available in the RefSeq database by January 2014
145 (**Supplementary Table S4**). For each genome, the retrieved homologs were designated as an RcGTA-like
146 head-tail cluster if at least 9 of the homologs had no more than 5,000 base pairs between any two adjacent
147 genes. The maximum distance cutoff was based on the observed distances between the neighboring
148 RcGTA head-tail cluster genes. This assignment was determined by clustering of the obtained homologs
149 with the DBSCAN algorithm (Ester et al. 1996) using an in-house Python script (available in a **GitHub**
150 repository; see **"Software Implementation"** section below). The resulting set of 88 "true GTAs" is
151 provided in **Supplementary Table S5**.

152 Since GTA functionality has been extensively studied only in *Rhodobacter capsulatus* SB1003
153 (Lang et al. 2017) and horizontal gene transfer likely occurred multiple times between the putative GTAs
154 and bacterial viruses (Hynes et al. 2016; Zhan et al. 2016), the bacterial homologs that were too divergent
155 from other bacterial RcGTA-like homologs were eliminated from the training sets to reduce possible
156 noise in classification. To do so, for each of the 11 trainings sets T^g, all detected viral and bacterial

157 homologs were aligned using MUSCLE v3.8.31 (Edgar 2004) and then pairwise phylogenetic distances
158 were estimated under PROTGAMMAJTT substitution model using RAxML version 8.2.11 (Stamatakis
159 2014). For each bacterial homolog in a set T^g, the pairwise phylogenetic distances between it and all
160 other bacterial homologs were averaged. This average distance was defined as an outlier distance (o) if it
161 satisfied the inequality:

162 $$o > Q_3 + 1.5 * (Q_3 - Q_1) \; (eq. 4)$$

163 where Q_1 and Q_3 are the first and third quartiles, respectively, of the distribution of the average distances
164 for all bacterial homologs in the training set T^g. If an outlier distance was greater than the shortest
165 distance from it to a viral homolog in the set T^g, the bacterial homolog was removed from the dataset.
166 The alignments, list of removed sequences and the associated calculations are available in the **FigShare**
167 repository.

168 Additionally, for each gene g, the sequences that had the same RefSeq ID (and therefore 100%
169 amino acid identity) were removed from the training data sets. The final number of sequences in each
170 training dataset are listed in **Table 1**.

171 **Assignment of weights to the training set sequences**

172 Highly similar training sequences can have an increased influence on the position of the
173 hyperplane, as misclassification of two or more similar sequences can be considered less optimal than
174 misclassification of only one sequence. To reduce such bias, a weighting scheme was introduced into the
175 soft-margin of the SVM classifier during training. First, sequences in each training set $T^g = \{T_1, \dots, T_m\}$
176 were aligned in MUSCLE v3.8.31 (Edgar 2004) (The alignments are available in the **FigShare**
177 repository). For each pair of sequences in a training set T^g, phylogenetic distances were calculated in
178 RAxML version 8.2.11 (Stamatakis 2014) under the best substitution model (PROTGAMMAAUTO; the
179 selected substitution matrices are listed in the **Supplementary Table S6**). The farthest-neighbor

180 hierarchical clustering method was used to group sequences with distances below a specified threshold t.
181 Weight d_i of each sequence in a group was defined as a reciprocal of the number of genes in the group.
182 These weights are used to adjust the cost of misclassification by multiplying C_{ii} for each sequence T_i by
183 d_i. The most suitable value of t was determined empirically during cross-validation, as described in the
184 **"Model training, cross validation, and assessment"** section below.

185 **Generation of sequence features**

186 To use amino acid sequences in the SVM classifier, each sequence was transformed to an *n*-
187 dimensional vector of compositional features. Three metrics that capture different aspects of sequence
188 composition were implemented: frequencies of "words" of size *k* (*k*-mers), pseudo amino-acid
189 composition (PseAAC), and physicochemical properties of amino acids.

190 In the first feature type, amino acid sequence of a gene is broken into a set of overlapping
191 subsequences of size *k*, and frequencies of these *n* unique *k*-mers form a feature vector $\boldsymbol{x}$. Values of *k*
192 equal to 2, 3, 4, 5 and 6 were evaluated for prediction accuracy (see the **"Model training, cross**
193 **validation, and assessment"** section below).

194 The second feature type, pseAAC, has n=(20+λ) dimensions and takes into account frequencies
195 of 20 amino acids, as well as correlations of hydrophobicity, hydrophilicity and side-chain mass of amino
196 acids that are λ positions apart in the sequence of the gene (after (Chou 2001)), More precisely, PseAAC
197 feature set $\boldsymbol{x}$ of a sequence of length *L* consisting of amino acids $R_1R_2\ldots R_L$ is defined as follows:

198
$$x_i = \begin{cases} \dfrac{r_i}{\sum_{i=1}^{20} r_i + \omega \sum_{k=1}^{\lambda} s_k}, & if\ 1 \le i \le 20, \\ \dfrac{\omega s_{j-20}}{\sum_{i=1}^{20} r_i + \omega \sum_{k=1}^{\lambda} s_k}, & if\ 21 \le j \le 20 + \lambda \end{cases} \qquad (eq.5)$$

where r_i is the frequency of the i-th amino acid (out of 20 possible), ω is a weight constant for the order effect that was set to 0.05, and s_k ($k = 1, \ldots, \lambda$) are sequence order-correlation factors. These factors are defined as

$$s_k = \frac{1}{L-k}\sum_{i=1}^{L-k} J_{i,i+k} \quad (eq.6)$$

where

$$J_{i,j} = \frac{1}{3}\left[\left(H1(Rj) - H1(Ri)\right)^2 + \left(H2(Rj) - H2(Ri)\right)^2 + \left(M(Rj) - M(Ri)\right)^2\right] \quad (eq.7)$$

and $H_1(R_i)$, $H_2(R_i)$, and $M(R_i)$ denote the hydrophobicity, hydrophilicity, and side-chain mass of amino acid R_i, respectively. The $H_1(R_i)$, $H_2(R_i)$, and $M(R_i)$ scores were subjected to a conversion as described in the following equation:

$$\begin{cases} H_1(i) = \dfrac{H_1^0(i) - \sum_{i=1}^{20}\frac{H_1^0(i)}{20}}{\sqrt{\dfrac{\sum_{i=1}^{20}\left[H_1^0(i) - \sum_{i=1}^{20}\frac{H_1^0(i)}{20}\right]^2}{20}}} \\ H_2(i) = \dfrac{H_2^0(i) - \sum_{i=1}^{20}\frac{H_2^0(i)}{20}}{\sqrt{\dfrac{\sum_{i=1}^{20}\left[H_2^0(i) - \sum_{i=1}^{20}\frac{H_2^0(i)}{20}\right]^2}{20}}} \\ M(i) = \dfrac{M^0(i) - \sum_{i=1}^{20}\frac{M^0(i)}{20}}{\sqrt{\dfrac{\sum_{i=1}^{20}\left[M^0(i) - \sum_{i=1}^{20}\frac{M^0(i)}{20}\right]^2}{20}}} \end{cases} \quad (eq.8),$$

209 where $H_1^0(i)$ is the original hydrophobicity value of the $i-th$ amino acid, $H_2^0(i)$ is hydrophilicity value,
210 and $M^0(i)$ is the mass of its side chain. Values of λ equal to 3 and 6 were evaluated for prediction
211 accuracy (see the **"Model training, cross validation, and assessment"** section below).

212 The third feature type relies on classification of amino acids into 19 overlapping classes of
213 physicochemical properties (**Supplementary Table S7**; after (Kaundal et al. 2013)). For a given
214 sequence, each of its encoded amino acids was counted towards one of the 19 classes, and the overall
215 scores for each class were normalized by the length of the sequence to form n = 19-dimensional feature
216 vector $\boldsymbol{x}$.

217 **Model training, cross validation, and assessment**

218 For each GTA gene, parameter, and feature type, the accuracy of the classifier was evaluated
219 using a five-fold cross-validation scheme, in which a dataset was randomly divided into five different
220 sub-samples. Four parts were combined to form the training set, while the fifth part was used as the
221 validation set and its SVM-assigned classifications compared to the known classes. This step was
222 repeated five times, so that every set was tested as a known class at least once. Results were evaluated by
223 their accuracy scores, defined as the number of correctly classified genes divided by the total number of
224 genes that were tested. The cross-validation procedure was repeated ten times to reduce the partitioning
225 bias, and the generated results were averaged to get the final assessment. Accuracy scores were weighted,
226 to ensure that "GTA" and "Virus" classes had equal impact, regardless of the size of each class. The most
227 suitable "softness" of the SVM margin was determined by trying all possible combinations of several raw
228 diagonal values of the matrix $\boldsymbol{C}$ (0.01, 0.1, 1, 100, 10000) and the threshold t (0, 0.01, 0.02, 0.03, 0.04,
229 0.05, 0.1). The set of parameters and features that resulted in the highest weighted accuracy was defined
230 as the optimal set for a gene g. If multiple parameter and feature sets resulted in the highest weighted
231 accuracy, we applied the following parameter selection criteria, in the priority order listed, until only one
232 parameter set was left: first, we selected parameter set(s) with k-mer size that on average performed better

233 than other *k*-mer sizes; second, we avoided parameter set(s) that included PseAAC and physicochemical
234 composition features; third, we selected parameter set(s) with the value of $\boldsymbol{C}$ that gives the highest average
235 accuracy across the remaining parameter sets; and finally, we opted for the parameter set with the value of
236 *t* that also gives the highest average accuracy across the remaining parameter sets.

237 Selection of alphaproteobacterial genomes for testing the presence of RcGTA-like genes

238 From the alphaproteobacterial genomes deposited to the RefSeq database between January 2014
239 and January 2019, we selected 636 complete and 789 high-quality draft genomes, with the latter defined
240 as genome assemblies with N50 length >400 kbp. The taxonomy of each genome was assigned using the
241 GTDB-Tk toolkit (Parks et al. 2018). The GTDB assignment is based on the combination of Average
242 Nucleotide Identity (Jain et al. 2018) and phylogenetic placement on the reference tree (as implemented in
243 the *pplacer* program (Matsen et al. 2010)). Three of the 1,425 genomes could not be reliably placed into a
244 known alphaproteobacterial order, and hence were left unclassified. Two of the 1,425 genomes were
245 removed from further analyses due to their classification outside of the Alphaproteobacteria class,
246 resulting in 635 complete and 788 high-quality genomes in our dataset (**Supplementary Table S8**).

247 Detection of RcGTA-like genes and head-tail clusters in Alphaproteobacteria

248 The compiled training datasets of the RcGTA-like genes (see the **"SVM training data"** section)
249 were used as queries in BLASTP (E-value < 0.001; query and subject overlap by at least 60% of their
250 length) searches of amino acid sequences of all annotated genes from the 1,423 alphaproteobacterial
251 genomes. Acquired homologs of unknown affiliation (sequences *u*) were then assigned to either "GTA" or
252 "virus" category by running the SVM classifier with the identified optimal parameters for each gene *g*
253 (**Table 2**).

254 The proximity of the individually predicted RcGTA-like genes in each genome was evaluated by
255 running the DBSCAN algorithm (Ester et al. 1996) implemented in an in-house Python script (available

256 in a **GitHub** repository; see **"Software Implementation"** section below). The retrieved homologs were
257 designated as an RcGTA-like head-tail cluster if at least 6 of the RcGTA-like genes had no more than
258 8,000 base pairs between any two adjacent genes. The maximum distance cutoff was increased from the
259 5,000 base pairs used for the clustering of homologs in the training datasets (see **"SVM Training Data"**
260 section) because the SVM classifier evaluates only 11 of the 17 RcGTA-like head-tail cluster homologs
261 and therefore the distances between some of the identified RcGTA-like genes can be larger.

262 To reduce the bias arising from the overrepresentation of particular taxa in the estimation of the RcGTA-
263 like cluster abundance in Alphaproteobacteria, the 1,423 genomes were grouped into Operational
264 Taxonomic Units (OTUs) by computing pairwise Average Nucleotide Identity (ANI) using the FastANI
265 v1.1 program (Jain et al. 2018) and defining boundaries between OTUs at the 95% threshold. Since not all
266 OTUs consist uniformly of genomes that were either all with or all without the RcGTA-like clusters, each
267 RcGTA-like cluster in an OTU was assigned a weight of "1/[number of genomes in an OTU]". The
268 abundance of the RcGTA-like clusters in different alphaproteobacterial orders was corrected by summing
269 up the weighted numbers of RcGTA-like clusters.

270 Software Implementation

271 The above described SVM classifier, generation of sequence features, and preparation and
272 weighting of training data are implemented in a Python program called "GTA-Hunter". The source code
273 of the program is available via GitHub at https://github.com/ecg-lab/GTA-Hunter-v1. The repository also
274 contains training data for the detection of the RcGTA-like heat-tail cluster genes, examples of how to run
275 the GTA-Hunter, and the script for clustering of the detected RcGTA-like genes using the DBSCAN
276 algorithm.

Assessment of prevalence of the RcGTA-like clusters among putative prophages

Putative prophages in the 1,423 alphaproteobacterial genomes were predicted using the PHASTER web server (Arndt et al. (2016); accessed in January, 2019). Only predicted prophages with the PHASTER score >90 (i.e., classified as "intact" prophages) were used in further analyses. The proportion of the predicted prophages classified by the GTA-Hunter as "GTA"s was calculated by comparing the overlap between the genomic locations of the predicted prophages and the putative RcGTA-like regions.

Construction of the alphaproteobacterial reference phylogeny

From the set of 120 phylogenetically informative proteins (Parks et al. 2017), 83 protein families that are present in a single copy in >95% of 1,423 alphaproteobacterial genomes were extracted using hmmsearch (E-value < 10^{-7}) via modified AMPHORA2 scripts (Wu and Scott 2012) (**Supplementary Table S9**). For each protein family, homologs from *Escherichia coli* str. K12 substr. DH10B and *Pseudomonas aeruginosa* PAO1 genomes (also retrieved using *hmmsearch*, as described above) were added to be used as an outgroup in the reconstructed phylogeny. The amino acid sequences of each protein family were aligned using MUSCLE v3.8.31 (Edgar 2004). Individual alignments were concatenated, keeping each alignment as a separate partition in further phylogenetic analyses (Chernomor et al. 2016). The most suitable substitution model for each partition was selected using *ProteinModelSelection.pl* script downloaded from https://github.com/stamatak/standard-RAxML/tree/master/usefulScripts. Gamma distribution with 4 categories was used to account for rate heterogeneity among sites (Yang 1994). The maximum likelihood phylogenetic tree was reconstructed with IQ-TREE v 1.6.7 (Nguyen et al. 2014). One thousand ultrafast bootstrap replicates were used to get support values for each branch (Hoang et al. 2017; Minh et al. 2013). The concatenated sequence alignment in PHYLIP format and the reconstructed phylogenetic tree in Newick format are available in the **FigShare** repository.

Examination of conditions associated with the decreased fitness of the knock-out mutants of the RcGTA-like head-tail cluster genes

From the three genomes that are known to contain RcGTA-like clusters (*Caulobacter crescentus* NA100, *Dinoroseobacter shibae* DFL-12, and *Phaeobacter inhibens* BS107), fitness experiments data associated with the knock-out mutants of the RcGTA-like head-tail cluster genes were retrieved from the Fitness Browser (Price et al. (2018); accessed in May, 2019 via http://fit.genomics.lbl.gov/cgi-bin/myFrontPage.cgi). Price et al. (2018) defined gene fitness as the log2 change in abundance of knock-out mutants in that gene during the experiment. For our analyses, the significantly decreased fitness of each mutant was defined as a deviation from the fitness of 0 with a $|t - score| \geq 4$. The conditions associated with the significantly decreased fitness were compared across the RcGTA-like head-tail cluster genes in all three genomes.

Results

GTA-Hunter is an effective way to distinguish RcGTA-like genes from their viral homologs

The performance of the developed SVM classifier depends on values of parameters that determine type and composition of sequence features, specify acceptable levels of misclassification, and account for biases in taxonomic representation of the sequences in the training sets. To find the most effective set of parameters, for each of the 11 RcGTA-like head-tail genes with the sufficient number of homologs available (**Figure 1**; also, see **Materials and Methods** for details) we evaluated the performance of 1,225 different combinations of the parameters using a cross-validation technique (**Supplementary Table S10**).

Generally, the classifiers that only use *k*-mers as the feature have higher median accuracies than the classifiers that solely rely either on physicochemical properties of amino acids or on pseudo amino

323 acid composition (PseAAC) (**Supplementary Figure S2** and **Supplementary Table S10**), indicating that
324 the conservation of specific amino acids blocks is important in delineation of RcGTA-like genes from
325 their viral counterparts. However, the accuracies are lower for the larger *k*-mer sizes (**Supplementary**
326 **Figure S2**), likely due to the feature vectors becoming too sparse. Consequently, parameter combinations
327 with values of *k* above 6 were not used. The lowest observed weighted accuracies involve usage of
328 physicochemical properties of proteins as a feature (**Supplementary Figure S2** and **Supplementary**
329 **Table S10**), suggesting the conservation of physicochemical properties of amino acids among proteins of
330 similar function in viruses and RcGTA-like regions despite their differences in the amino acid
331 composition. The more sophisticated re-coding of physicochemical properties of amino acids as the
332 PseAAC feature performs better, but for all genes its performance is worse than the best-performing *k*-
333 mer (**Supplementary Figure S2** and **Supplementary Table S10**).

334 For several genes, the maximum weighted accuracy was obtained with multiple combinations of
335 features and parameter values (**Supplementary Table S10**). Based on the above-described observations
336 of the performance of individual features, we preferred parameter sets that did not include PseAAC and
337 physicochemical composition features, and selected *k*-mer size that on average performed better than
338 other *k*-mer sizes (see **Materials and Methods** for the full description of the parameter selection
339 procedure).

340 For individual genes, the maximum achieved weighted accuracy ranges from 95.6 to 100%
341 (**Table 2**), with 5 out of 11 genes reaching 100% prediction accuracy. The two genes with the maximum
342 weighted accuracy below 99% (*g6* and *g12*) also have the smallest number of viral homologs available for
343 training, which is a likely cause for the reduced classifier efficacy. Additionally, several viral homologs in
344 the training datasets for *g6* and *g12* genes have smaller phylogenetic distances to "true GTA" homologs
345 than to other "true virus" homologs (**Supplementary Table S11**). As a result, due to the unequal sizes of
346 "true virus" and "true GTA" datasets (**Table 1**) and the usage of weighted accuracies to correct for that,

347 the SVM classifier based on the best set of parameters (**Table 2**) erroneously classifies some of the
348 RcGTA-like *g6* and *g12* genes (**Supplementary Table S10**).

349 For each gene, the identified most accurate parameter set (**Table 2**) was used to classify homologs
350 of the RcGTA genes in the 1,423 alphaproteobacterial genomes (**Supplementary Table S8**).

351 GTA-Hunter predicts abundance of RcGTA-like head-tail clusters in Alphaproteobacteria

352 The 1,423 examined alphaproteobacterial genomes contain 7,717 homologs of the 11 RcGTA
353 genes. The GTA-Hunter classified 6,045 of these homologs as "GTA" genes (**Supplementary Table**
354 **S12**). From this analysis alone, however, we do not know if these putative GTA genes are located in the
355 same neighborhood in a genome. Although in the *Rhodobacter capsulatus* genome the genes encoding
356 RcGTA are distributed across at least 5 loci, the head-tail cluster genes are found in one locus (Hynes et
357 al. 2016). Therefore, in our analyses we imposed an extra requirement of the predicted RcGTA-like head-
358 tail cluster genes to be in proximity on the chromosome. Additionally, since there is at least one known
359 case of horizontal gene transfer of GTA genes into a virus (Zhan et al. 2016), we also required the putative
360 RcGTA-like cluster to consist of at least 6 of the 11 tested genes. This procedure revealed that RcGTA-
361 like clusters are present in one (and only one) copy in 818 of the 1,423 (~57.5%) examined
362 alphaproteobacterial genomes (**Supplementary Table S13** and **Table 3**). Uneven taxonomic
363 representation of Alphaproteobacteria among the analyzed genomes may inflate this estimation of the
364 abundance of the GTA-harboring genomes within the class. To correct for this potential bias, 1,423
365 genomes were grouped into 797 Operational Taxonomic Units (OTUs) based on the average nucleotide
366 identity (ANI) of their genomes (**Supplementary Table S14**). Although indeed some taxonomic groups
367 are overrepresented in the set of 1,423 genomes, in 450 of the 797 OTUs (56.4%) all OTU members
368 contain the putative RcGTA-like clusters (**Supplementary Table S14**).

369 **RcGTA-like clusters are widely distributed within a large sub-clade of Alphaproteobacteria**

370 The 818 genomes with the RcGTA-like gene clusters detected in this study are not evenly
371 distributed across the class (**Table 3**), but are found only in a clade that includes seven orders (clade 4 in
372 **Figure 3**). Overall, 66% of the examined OTUs within the clade 4 are predicted to have an RcGTA-like
373 cluster (**Table 3**). RcGTA-like clusters are most abundant in clade 6 (**Figure 3**), a group that consists of
374 the orders *Rhodobacterales* and *Caulobacterales* (**Table 3**).

375 Although the two unclassified orders that contain RcGTA-like clusters are represented by only
376 two genomes (clades 2 and 3 in **Figure 3**), their position on the phylogenetic tree of Alphaproteobacteria
377 suggests that the RcGTA-like element may have originated earlier than was proposed by Shakya et al.
378 (2017) (clade 5 on **Figure 3**). Given that RcGTA-like head-tail cluster genes are readily detectable in viral
379 genomes, it is unlikely that the RcGTA-like clusters remained completely undetectable in the examined
380 genomes outside of the clade 4 due to the sequence divergence. Therefore, an RcGTA-like element was
381 unlikely to be present in the last common ancestor of all Alphaproteobacteria (clade 7 on **Figure 3**),
382 which was suggested when only a limited number of genomic data was available (Lang and Beatty 2007).

383 **Most of the detected RcGTA-like clusters can be mistaken for prophages**

384 Among the 818 detected RcGTA-like clusters, the functional annotations of the 11 examined
385 genes were similar to the prophages and none of them refer to a "gene transfer agent" (data not shown).
386 Since at least 11 of the 17 RcGTA head-tail cluster genes have detectable sequence similarity to viral
387 genes (**Supplementary Table S3**), it is likely that, if not recognized as GTAs, many of the putative
388 RcGTA-like clusters will be designated as "prophages" in genome-wide searches of prophage-like
389 regions. Indeed, of the 1,235 'intact' prophage regions (see **Materials and Methods** for definition)
390 predicted in the clade 4 genomes, 664 (54%) coincide with the RcGTA-like clusters (**Figure 4**).
391 Conversely, 664 out of 818 of the predicted RcGTA-like clusters (81%) are classified as intact prophages.

392 Of the 351 RcGTA-like clusters that contain *all* 11 examined genes, 323 (92%) are classified as intact
393 prophages.

394 Interestingly, within 818 genomes that contain RcGTA-like clusters, the average number of
395 predicted intact prophages is 1.23 per genome (**Figure 5**), which is significantly higher than 0.51
396 prophages per genome in genomes not predicted to contain RcGTA-like clusters (p-value $< 0.22 * 10^{-17}$;
397 Mann-Whitney U test). If the 664 RcGTA-like regions classified as intact prophages are removed from
398 the genomes that contain them, the average number of predicted 'intact' prophages per genome drops to
399 0.42 (**Figure 5**) and the difference becomes insignificant (p-value = 0.1492; Mann-Whitney U test). This
400 analysis suggests that an elevated number of the observed predicted prophage-like regions in some
401 alphaproteobacterial genomes may be due to the presence of unrecognized RcGTA-like elements.

402

403 Discussion

404 Our study demonstrates that RcGTA-like and *bona fide* viral homologs can be clearly separated
405 from each other using a machine learning approach. The highest accuracy of the classifier is achieved
406 when it primarily relies on short amino acid *k*-mers present in the examined genes. This suggests that the
407 distinct primary amino acid composition of the RcGTA-like and truly viral proteins is what allows the
408 separation of the two classes of elements (**Figure 1**). However, the cause of the amino acid preferences of
409 the RcGTA-like genes, and especially enrichment of the encoded proteins in alanine and glycine amino
410 acids (**Figure 1**), remains unknown. Given the structure of the genetic code, the skewed amino acid
411 composition may be the driving force behind the earlier described significantly higher %G+C of the
412 genomic region encoding the RcGTA-like head-tail cluster than the average %G+C in the host genome
413 (Shakya et al. 2017). Regardless of the cause of the skewed amino acid composition, the successful
414 identification of RcGTA-like elements in alphaproteobacterial taxa only distantly related to *Rhodobacter*

415 *capsulatus* (clade 4 in **Figure 3**) suggests that the selection to maintain these elements likely extends
416 beyond the *Rhodobacterales* order.

417 However, the benefits associated with the GTA production that would underly the selection to
418 maintain them remain unknown. In a recently published high-throughput screen for phenotypes associated
419 with specific genes (Price et al. 2018), knockout of the RcGTA-like genes in the three genomes that
420 encode the RcGTA-like elements resulted in decreased fitness of the mutants (in comparison to the wild
421 type) under some of the tested conditions (**Supplementary Table S15**). Interestingly, the conditions
422 associated with the most statistically significant decreases in fitness correspond to the growth on non-
423 glucose sugars, such as D-Raffinose, β-Lactose, D-Xylose and m-Inositol. Overall, carbon source
424 utilization is the most common condition that elicits statistically significant fitness decreases in the
425 mutants. The RcGTA production was also experimentally demonstrated to be stimulated by carbon
426 depletion (Westbye et al. 2017). Further experimental work is needed to identify the link between the
427 RcGTA-like genes expression and carbon utilization. Conversely, absence of the RcGTA-like elements in
428 some of the clade 4 genomes (**Figure 3**) indicates that in some ecological settings RcGTA-like elements
429 are either deleterious or "useless" and thus their genes were either purged from the host genomes (if
430 RcGTA-like element evolution is dominated by vertical inheritance) or not acquired (if horizontal gene
431 transfer plays a role in the RcGTA-like element dissemination).

432 Previous analyses inferred that RcGTA-like elements had evolved primarily vertically, with few
433 horizontal gene exchanges between closely related taxa (Hynes et al. 2016; Lang and Beatty 2007;
434 Shakya et al. 2017). Under this hypothesis, the distribution of the RcGTA-like head-tail clusters in
435 alphaproteobacterial genomes suggests that RcGTA-like element originated prior to the last common
436 ancestor of the taxa in clade 4 (**Figure 3**). This places the origin of the RcGTA-like element to even
437 earlier timepoint than the one proposed in Shakya et al. (2017). However, it should be noted that our
438 inference is sensitive to the correctness of the inferred relationships of taxa within the
439 alphaproteobacterial class, which remain to be disputed due to compositional biases and unequal rates of

440 evolution of some alphaproteobacterial lineages (Munoz-Gomez et al. 2019). The most recent
441 phylogenetic inference that takes into account these heterogeneities (Munoz-Gomez et al. 2019) is
442 different from the reference phylogeny shown in **Figure 3**. Relevant to the evolution of RcGTA-like
443 elements, on the phylogeny in Munoz-Gomez et al.(2019) the order Pelagibacterales is located within the
444 clade 4 instead of being one of the early-branching alphaproteobacterial orders (**Figure 3**). No RcGTA-
445 like clusters were detected in Pelagibacterales, although in our analyses the order is represented by only
446 five genomes. Better sampling of genomes within this order would be needed either to show a loss of the
447 RcGTA-like element in this order or to re-assess the hypothesis about origin and transmission of the
448 RcGTA-like elements within Alphaproteobacteria.

449 Genes in the detected RcGTA-like head-tail clusters remain mainly unannotated as "gene transfer
450 agents" in GenBank records, and therefore they can be easily confused with prophages. For example,
451 recently described "conserved prophage" in *Sphingomonadales* (Viswanathan et al. 2017) is predicted to
452 be an RcGTA-like element by GTA-Hunter. Incorporation of a GTA-Hunter-like machine learning
453 classification into an automated genome annotation pipeline will help improve quality of the gene
454 annotations in GenBank records and facilitate discovery of GTA-like elements in other taxa. Moreover,
455 application of the presented GTA-Hunter program is not limited to the detection of the RcGTA-like
456 elements. With appropriate training datasets, the program can be applied to the detection of GTAs that do
457 not share evolutionary history with the RcGTA (Lang et al. 2017) and of other elements that are
458 homologous to viruses or viral sub-structures, such as type VI secretion system (Leiman et al. 2009),
459 encapsulins (Giessen and Silver 2017).

460

Acknowledgements

This work was supported by the National Science Foundation [NSF-DEB 1551674 to O.Z.]; the Simons Foundation Investigator in Mathematical Modeling of Living Systems [327936 to O.Z.]; Dartmouth Dean of Faculty start-up funds to O.Z.; and Dartmouth James O. Freedman Presidential Scholarship to T.N.

Tables

Table 1. Number of the RcGTA homologs in the "true GTA" and "true virus" training datasets.

Gene	"true GTAs"	"true viruses"
g2	69	1646
g3	65	769
g4	62	465
g5	67	627
g6	61	19
g8	62	96
g9	66	61
g12	63	12
g13	73	57
g14	67	124
g15	67	155

469 **Table 2. The combinations of features and parameters that showed the highest accuracy in cross-**

470 **validation.** The listed parameter sets were used in predictions of the RcGTA-like genes in 1,423

471 alphaproteobacterial genomes. See **Materials and Methods** for the procedure on selecting one parameter

472 set in the cases where multiple parameter sets had the same highest accuracy.

473

Gene	**Accuracy (%)**	**k-mer (size)**	**PseAAC** (value of **λ**)	**Grouping based on physicochemical properties of amino acids**	***C***	***T***
g2	100	2	-[1]	-	10000	0.02
g3	100	3	-	-	10000	0.02
g4	100	3	3	-	10000	0.02
g5	100	3	-	-	100	0.02
g6	95.9	4	-	+	0.1	0.02
g8	99.4	2	3	-	0.1	0.03
g9	100	2	-	-	100	0.1
g12	95.6	5	-	-	10000	0.05
g13	99.1	2	-	-	100	0
g14	99.6	6	6	-	0.01	0.03
g15	99.7	2	-	-	10000	0.02

474 [1] throughout the table, "-" denotes that the feature type was not used

475

476 **Table 3. Distribution of prophages and RcGTA-like elements across different orders within class**

477 **Alphaproteobacteria.**

Order	Number of genomes	Number of prophages	Number of RcGTA-like clusters	Number of OTUs	Corrected abundance of RcGTA-like clusters[1]	Percentage of OTUs that have RcGTA-like clusters
Acetobacterales	62	34	0	34	0	0
Azospirillales	13	10	0	12	0	0
Caedibacterales	1	0	0	1	0	0
Caulobacterales	50	30	39	45	35	78
Elsterales	1	0	0	1	0	0
Kiloniellales	5	1	0	3	0	0
Oceanibaculales	2	1	0	2	0	0
Paracaedibacterales	1	2	0	1	0	0
Parvibaculales	5	5	2	5	2	40
Pelagibacterales	5	0	0	5	0	0
Rhizobiales	730	763	435	300	155	52
Rhodobacterales	241	318	208	174	150	86
Rhodospirillales	24	10	0	15	0	0
Rickettsiales	70	18	0	24	0	0
Sneathiellales	2	1	0	2	0	0
Sphingomonadales	207	115	132	169	110	65
Thalassobaculales	1	0	0	1	0	0
Unclassified order 1	1	0	0	1	0	0
Unclassified order 2	1	2	1	1	1	100
Unclassified order 3	1	2	1	1	1	100

478 [1] See "**Detection of RcGTA-like genes and head-tail clusters in Alphaproteobacteria"** subsection of

479 the **Materials and Methods** for explanation about the correction.

480

481 # Figure Legends

482 **Figure 1. The 'head-tail' cluster of the *Rhodobacter capsulatus* GTA "genome" and the amino acid**
483 **composition of viral and alphaproteobacterial homologs for some of its genes.** Genes that are used in
484 the machine learning classification are highlighted in grey. For those genes, the heatmap below a gene
485 shows the relative abundance of each amino acid (rows) averaged across the RcGTA-like and viral
486 homologs that were used in the classifier training (columns). The heatmaps of the amino acid composition
487 in the individual homologs are shown in **Supplementary Figure S1**.

488

489 **Figure 2. The pseudocode of the SVM classifier algorithm that distinguishes RcGTA-like genes**
490 **from the 'true' viruses.** The algorithm is implemented in the GTA-Hunter software package (see
491 **"Software Implementation"** section in **Materials and Methods**).

492

493 **Figure 3. Distribution of the detected RcGTA-like clusters across the class Alphaproteobacteria.**
494 The presence of RcGTA-like clusters is mapped to a reference phylogenetic tree that was reconstructed
495 from a concatenated alignment of 83 marker genes (See **Materials and Methods** and **Supplementary**
496 **Table S9**). The branches of the reference tree are collapsed at the taxonomic rank of "order", and the
497 number of OTUs within the collapsed clade is shown in parentheses next to the order name. Orange and
498 brown bars depict the proportion of OTUs with and without the predicted RcGTA-like clusters,
499 respectively. The orders that contain at least one OTU with an RcGTA-like cluster are colored in green.
500 Nodes 1, 2 and 3 mark the last common ancestors of the unclassified orders. Node 4 marks the lineage
501 where, based on this study, the RcGTA-like element should have already been present. Nodes 5 and 7
502 mark the lineages that were previously inferred to represent last common ancestor of the RcGTA-like
503 element by Shakya et al. (2017) and Lang and Beatty (2007), respectively. Node 6 marks the clade where

504 RcGTA-like elements are the most abundant. The tree is rooted using homologs from *Escherichia coli* str.
505 K12 substr. DH10B and *Pseudomonas aeruginosa* PAO1 genomes. Branches with ultrafast bootstrap
506 values >= 95% are marked with black circles. The scale bar shows the number of substitutions per site.
507 The full reference tree is provided in the **FigShare** repository.

508

509 **Figure 4. An overlap between prophage and GTA predictions.** The "predicted RcGTA-like clusters"
510 set refers to the GTA-Hunter predictions, while the "predicted intact prophages" set denotes predictions
511 made by the PHASTER program (Arndt et al. 2016) on the subset of the genomes that are found within
512 clade 4 (**Figure 3**).

513

514 **Figure 5. The number of predicted 'intact' prophages in alphaproteobacterial genomes.** The 1,423
515 genomes were divided into two groups: those without GTA-Hunter-predicted RcGTA-like clusters (in
516 brown) and those with these RcGTA-like clusters (in dark orange). For the latter group, the number of
517 prophages was re-calculated after the RcGTA-like clusters that were designated as prophages were
518 removed (in light orange). The distribution of the number of predicted intact prophages within each
519 dataset is shown as a violin plot with the black point denoting the average value. The datasets with
520 significantly different average values are denoted by asterisks ($p < 0.001$; Mann-Whitney U test).

521

522 Supplementary Figure Legends and Table Captions

523 **Supplementary Figure S1.** The amino acid composition of viral and alphaproteobacterial homologs of
524 the 11 RcGTA genes. These homologs were used in the training and cross-validation of the SVM
525 classifier. Each heatmap corresponds to one of the 11 genes (see **Supplementary Table S1** for the

526 functional annotations of the genes). Each row in a heatmap corresponds to an individual homolog of the
527 RcGTA gene. The homologs from viruses and alphaproteobacterial are separated by the black line and
528 labeled as “True Virus” and “True GTA”, respectively. The heatmap shows the relative abundance of
529 each amino acid within a homolog.

530

531 **Supplementary Figure S2. The weighted accuracies for different types of features.** The boxplots for
532 the three feature types are color coded. The data for five examined *k*-mer sizes (2, 3, 4, 5, 6) are shown
533 from the left to the right on the graphs. Each boxplot shows a median value bounded by the first and third
534 quartiles, and the whiskers depict a deviation that was calculated using the 1.5*InterQuartile Range rule.
535 Outliers are shown as dots.

536

537 **Supplementary Table S1. Functional annotations of the 'head-tail' cluster genes of the *Rhodobacter***
538 ***capsulatus* gene transfer agent.**

539

540 **Supplementary Table S2. List of the 7,995 viral assemblies used to find RcGTA homologs for the**
541 **training datasets.**

542

543 **Supplementary Table S3. List of 1,939 viruses with at least one detected RcGTA homolog.** The data
544 in the columns show the accession numbers of these homologs.

545

546 **Supplementary Table S4. List of 235 alphaproteobacterial genomes used to find large RcGTA-like**
547 **clusters for the training datasets.**

548

549 **Supplementary Table S5. List of 88 alphaproteobacterial RcGTA-like clusters detected in 85**
550 **genomes.** The data in the columns show the accession numbers of these homologs.

551

552 **Supplementary Table S6. Selected substitution matrices that were used to generate pairwise**
553 **phylogenetic distances within training datasets.**

554

555 **Supplementary Table S7. Grouping of amino acids into classes based on their physicochemical**
556 **properties (after Kaundal et al., 2013).**

557

558 **Supplementary Table S8. List of 1,423 alphaproteobacterial genomes used for testing the presence**
559 **of RcGTA-like genes.**

560

561 **Supplementary Table S9. Information about 83 marker genes that were used to reconstruct**
562 **reference phylogeny of Alphaproteobacteria.**

563

564 **Supplementary Table S10. Summary of the classifier cross-validation.** Results for each gene are
565 shown in separate tabs. Each row represents one of the 1,225 tested combinations of the parameters
566 (columns A-E), number of correctly classified homologs averaged across 10 replicates (columns F and G),
567 and the overall weighted accuracy of the parameter combination (column H). When a feature was not
568 used, the value of the parameter shown in columns A-C is set to 0.

569

570 **Supplementary Table S11. Phylogenetic distances of the "truly viral" homologs of the genes g6 and**
571 **g12 to "true GTAs" and to other "true viruses" in the training datasets.** Data for the g6 and g12
572 homologs are shown in separate tabs. Viral homologs that are more closely related to "true GTAs" than to
573 other "true viruses" are highlighted in yellow.

574

575 **Supplementary Table S12. Summary of the alphaproteobacterial RcGTA homologs' classification.**

576

577 **Supplementary Table S13. Information about the 818 detected RcGTA-like clusters. Data in**
578 **columns D-N correspond to the RefSeq accession numbers of the encoded proteins.**

579

580 **Supplementary Table S14. Presence of the RcGTA-like clusters in the reconstructed**
581 **alphaproteobacterial Operational Taxonomic Units (OTUs).**

582

583 **Supplementary Table S15. Results of the fitness experiments with the knock-out mutants of the**
584 **RcGTA-like head-tail cluster genes in three alphaproteobacterial genomes.** The data was retrieved
585 from the Fitness Browser (Price et al 2018). Each row corresponds to a separate experiment, in which the
586 specified gene was knocked out (column B) and decreased fitness (columns E and F) was associated with
587 a specific condition (column D). The conditions are classified into groups (column C). Rows
588 corresponding to the "carbon source" group are highlighted in yellow. This group is the most common
589 among the listed experiments and is found in experiments associated with each of the three genomes. For
590 description of conditions, refer to the Fitness Browser (Price et al 2018).

591

References

Altschul SF, et al. 1997. Gapped BLAST and PSI-BLAST: a new generation of protein database search programs. Nucleic Acids Res 25: 3389-3402.

Andersen M, Dahl J, Liu Z, Vandenberghe L. 2012. Interior-point methods for large-scale cone programming. In: Sra S, Nowozin S, Wright SJ, editors. Optimization for Machine Learning: MIT Press. p. 55–83.

Arndt D, et al. 2016. PHASTER: a better, faster version of the PHAST phage search tool. Nucleic Acids Res 44: W16-W21.

Bhardwaj N, Langlois RE, Zhao G, Lu H. 2005. Kernel-based machine learning protocol for predicting DNA-binding proteins. Nucleic Acids Res 33: 6486-6493.

Chernomor O, von Haeseler A, Minh BQ. 2016. Terrace aware data structure for phylogenomic inference from supermatrices. Syst Biol 65: 997-1008.

Chou KC. 2001. Prediction of protein cellular attributes using pseudo-amino acid composition. Proteins 43: 246-255.

Cortes C, Vapnik V. 1995. Support-vector networks. Mach Learn 20: 273-297.

Edgar RC. 2004. MUSCLE: multiple sequence alignment with high accuracy and high throughput. Nucleic Acids Res 32: 1792-1797.

Ester M, Kriegel H-P, Sander J, Xu X. 1996. A density-based algorithm for discovering clusters a density-based algorithm for discovering clusters in large spatial databases with noise. In Simoudis E, Han J, Fayyad U editors. *Proceedings of the Second International Conference on Knowledge Discovery and Data Mining*: 3001507: AAAI Press. p. 226-231.

Fu Y, et al. 2010. High diversity of *Rhodobacterales* in the subarctic North Atlantic Ocean and gene transfer agent protein expression in isolated strains. Aquat Microb Ecol 59: 283-293.

Giessen TW, Silver PA. 2017. Widespread distribution of encapsulin nanocompartments reveals functional diversity. Nat Microbiol 2: 17029.

Grull MP, Mulligan ME, Lang AS. 2018. Small extracellular particles with big potential for horizontal gene transfer: membrane vesicles and gene transfer agents. FEMS Microbiol Lett 365.

Hoang DT, Chernomor O, Von Haeseler A, Minh BQ, Vinh LS. 2017. UFBoot2: improving the ultrafast bootstrap approximation. Mol Biol Evol 35: 518-522.

Hynes AP, Mercer RG, Watton DE, Buckley CB, Lang AS. 2012. DNA packaging bias and differential expression of gene transfer agent genes within a population during production and release of the *Rhodobacter capsulatus* gene transfer agent, RcGTA. Mol Microbiol 85: 314-325.

Hynes AP, et al. 2016. Functional and evolutionary characterization of a gene transfer agent's multilocus "genome". Mol Biol Evol 33: 2530-2543.

Jain C, Rodriguez-R LM, Phillippy AM, Konstantinidis KT, Aluru S. 2018. High throughput ANI analysis of 90K prokaryotic genomes reveals clear species boundaries. Nat Commun 9: 5114.

Karchin R, Karplus K, Haussler D. 2002. Classifying G-protein coupled receptors with support vector machines. Bioinformatics 18: 147-159.

Kaundal R, Sahu SS, Verma R, Weirick T. 2013. Identification and characterization of plastid-type proteins from sequence-attributed features using machine learning. BMC Bioinformatics 14: S7.

Keen EC. 2015. A century of phage research: bacteriophages and the shaping of modern biology. Bioessays 37: 6-9.

Koonin EV, Krupovic M. 2018. The depths of virus exaptation. Curr Opin Virol 31: 1-8.

Lang AS, Beatty JT. 2007. Importance of widespread gene transfer agent genes in alpha-proteobacteria. Trends Microbiol 15: 54-62.

Lang AS, Westbye AB, Beatty JT. 2017. The distribution, evolution, and roles of gene transfer agents in prokaryotic genetic exchange. Ann Rev Virol 4: 87-104.

639 Lang AS, Zhaxybayeva O, Beatty JT. 2012. Gene transfer agents: phage-like elements of genetic
640 exchange. Nat Rev Microbiol 10: 472.
641 Leiman PG, et al. 2009. Type VI secretion apparatus and phage tail-associated protein complexes share a
642 common evolutionary origin. Proc Natl Acad Sci U S A 106: 4154-4159.
643 Marrs B. 1974. Genetic recombination in *Rhodopseudomonas capsulata*. Proc Natl Acad Sci USA 71:
644 971-973.
645 Matsen FA, Kodner RB, Armbrust EV. 2010. pplacer: linear time maximum-likelihood and Bayesian
646 phylogenetic placement of sequences onto a fixed reference tree. BMC Bioinformatics 11: 538.
647 Minh BQ, Nguyen MAT, von Haeseler A. 2013. Ultrafast approximation for phylogenetic bootstrap. Mol
648 Biol Evol 30: 1188-1195.
649 Munoz-Gomez SA, et al. 2019. An updated phylogeny of the *Alphaproteobacteria* reveals that the
650 parasitic *Rickettsiales* and *Holosporales* have independent origins. Elife 8.
651 Nagao N, et al. 2015. The gene transfer agent-like particle of the marine phototrophic bacterium
652 *Rhodovulum sulfidophilum*. Biochem Biophys Rep 4: 369-374.
653 Nguyen L-T, Schmidt HA, von Haeseler A, Minh BQ. 2014. IQ-TREE: a fast and effective stochastic
654 algorithm for estimating maximum-likelihood phylogenies. Mol Biol Evol 32: 268-274.
655 Parks DH, et al. 2018. A standardized bacterial taxonomy based on genome phylogeny substantially
656 revises the tree of life. Nat Biotechnol 36: 996-1004.
657 Parks DH, et al. 2017. Recovery of nearly 8,000 metagenome-assembled genomes substantially expands
658 the tree of life. Nat Microbiol 2: 1533.
659 Price MN, et al. 2018. Mutant phenotypes for thousands of bacterial genes of unknown function. Nature
660 557: 503.
661 Shakya M, Soucy SM, Zhaxybayeva O. 2017. Insights into origin and evolution of α-proteobacterial gene
662 transfer agents. Virus Evol 3: vex036.
663 Stamatakis A. 2014. RAxML version 8: a tool for phylogenetic analysis and post-analysis of large
664 phylogenies. Bioinformatics 30: 1312-1313.
665 Tomasch J, et al. 2018. Packaging of *Dinoroseobacter shibae* DNA into gene transfer agent particles is
666 not random. Genome Biol Evol 10: 359-369.
667 Touchon M, Bernheim A, Rocha EP. 2016. Genetic and life-history traits associated with the distribution
668 of prophages in bacteria. ISME J 10: 2744.
669 Viswanathan V, Narjala A, Ravichandran A, Jayaprasad S, Siddaramappa S. 2017. Evolutionary
670 Genomics of an Ancient Prophage of the Order *Sphingomonadales*. Genome Biol Evol 9: 646-
671 658.
672 Westbye AB, O'Neill Z, Schellenberg-Beaver T, Beatty JT. 2017. The *Rhodobacter capsulatus* gene
673 transfer agent is induced by nutrient depletion and the RNAP omega subunit. Microbiol 163:
674 1355-1363.
675 Wu M, Scott AJ. 2012. Phylogenomic analysis of bacterial and archaeal sequences with AMPHORA2.
676 Bioinformatics 28: 1033-1034.
677 Xu B, Tan Z, Li K, Jiang T, Peng Y. 2017. Predicting the host of influenza viruses based on the word
678 vector. PeerJ 5: e3579.
679 Yang Z. 1994. Maximum likelihood phylogenetic estimation from DNA sequences with variable rates
680 over sites: approximate methods. J Mol Evol 39: 306-314.
681 Zhan Y, Huang S, Voget S, Simon M, Chen F. 2016. A novel roseobacter phage possesses features of
682 podoviruses, siphoviruses, prophages and gene transfer agents. Sci Rep 6: 30372.
683

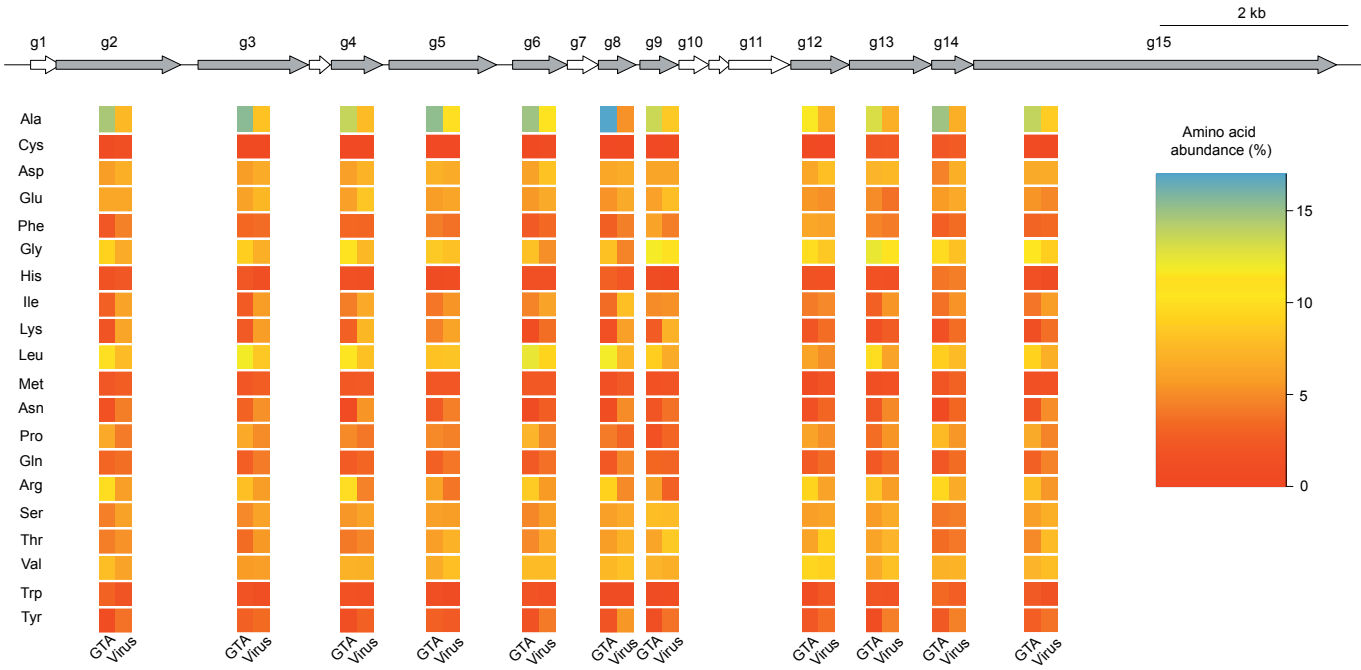

Figure 1. The 'head-tail' cluster of the Rhodobacter capsulatus GTA "genome" and the amino acid composition of viral and alphaproteobacterial homologs for some of its genes. Genes that are used in the machine learning classification are highlighted in grey. For those genes, the heatmap below a gene shows the relative abundance of each amino acid (rows) averaged across the RcGTA-like and viral homologs that were used in the classifier training (columns). The heatmaps of the amino acid composition in the individual homologs are shown in Supplementary Figure S1.

Let $T = (T_1, \ldots, T_m)$ be an array of training sequences $T_i, 1 \leq i \leq m$

Let $X = (x_i)$ be the feature sets for genes $T_i \in T$

Let $Y = (y_i)$ be the classes for genes $T_i \in T$

Let $W = (d_i)$ be the weights for genes $T_i \in T$

Let $y_i = -1$ if T_i is a GTA and $y_i = 1$ if it is a virus

Let $QUADPROG$ be a quadratic programming solver

procedure $SVMTrain(T, C)$

    $Compute\ Lagrange - multipliers = QUADPROG(X, Y, C * W)$

    Let $alphas = \{\alpha_i \in Lagrange - multipliers : \alpha_i > 10^{-5}\}$

    Let $support\ vectors = \{T_i \in Lagrange - multipliers : \alpha_i > 10^{-5}\}$

    return $alphas,\ support\ vectors$

end procedure

Let u be an unclassified gene, where x_u is the feature set of u

procedure $SVMPredict(alphas,\ supportvectors,\ x_u)$

    Let $score = 0$

    for $\alpha_i \in alphas\ and\ T_i \in support\ vectors$ **do**

        $score = score + (\alpha_i * y_i * K(x_i * x_u))$

    end for

    if $score < 0$ **then**

        return "GTA"

    else

        return "virus"

    end if

end procedure

Figure 2. The pseudocode of the SVM classifier algorithm that distinguishes RcGTA-like genes from the 'true' viruses. The algorithm is implemented in the GTA-Hunter software package.

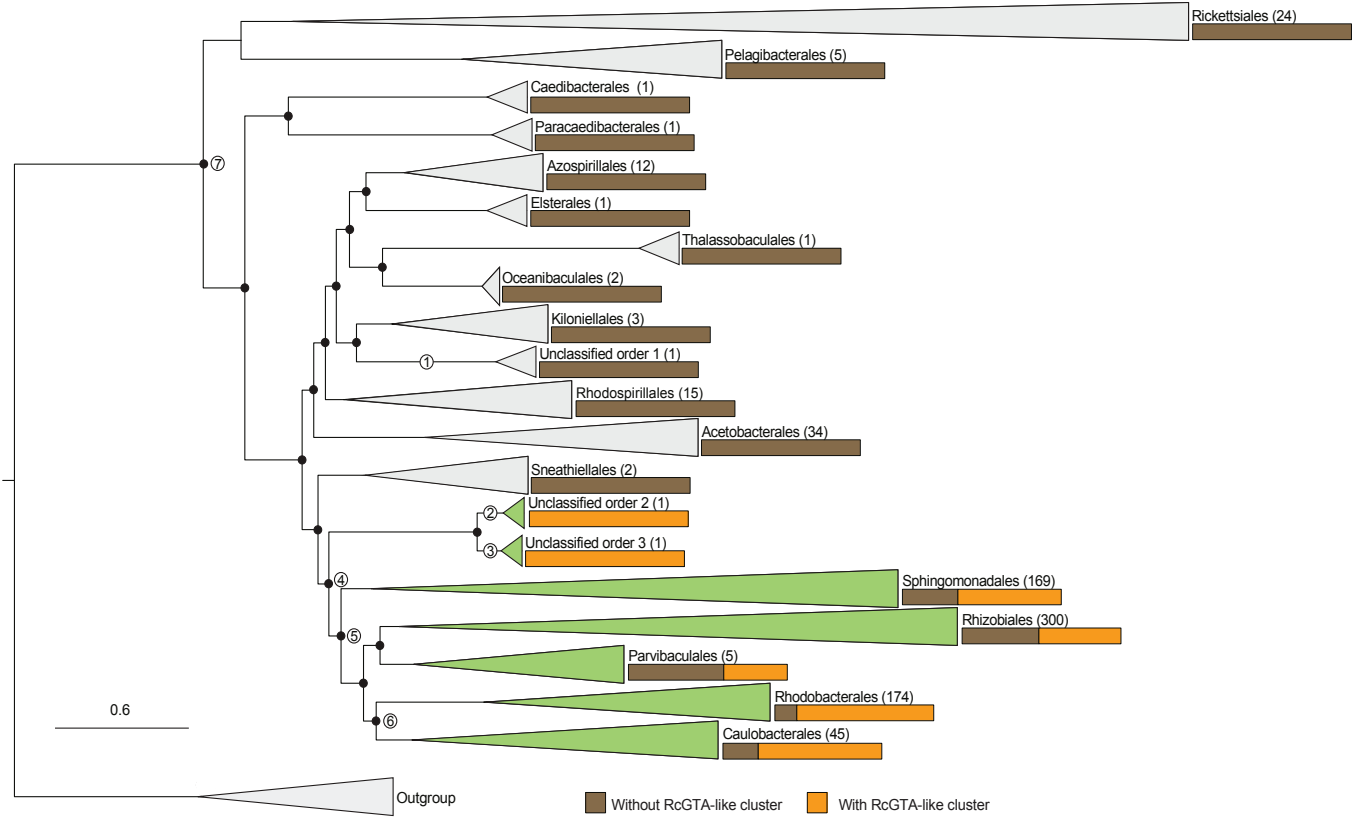

Figure 3. Distribution of the detected RcGTA-like clusters across the class Alphaproteobacteria. The presence of RcGTA-like clusters is mapped to a reference phylogenetic tree that was reconstructed from a concatenated alignment of 83 marker genes (See Materials and Methods and Supplementary Table S9). The branches of the reference tree are collapsed at the taxonomic rank of "order", and the number of OTUs within the collapsed clade is shown in parentheses next to the order name. Orange and brown bars depict the proportion of OTUs with and without the predicted RcGTA-like clusters, respectively. The orders that contain at least one OTU with an RcGTA-like cluster are colored in green. Nodes 1, 2 and 3 mark the last common ancestors of the unclassified orders. Node 4 marks the lineage where, based on this study, the RcGTA-like element should have already been present. Nodes 5 and 7 mark the lineages that were previously inferred to represent last common ancestor of the RcGTA-like element by (Shakya et al. 2017) and (Lang and Beatty 2007), respectively. Node 6 marks the clade where RcGTA-like elements are the most abundant. The tree is rooted using homologs from Escherichia coli str. K12 substr. DH10B and Pseudomonas aeruginosa PAO1 genomes. Branches with ultrafast bootstrap values >= 95% are marked with black circles. The scale bar shows the number of substitutions per site. The full reference tree is provided in the FigShare repository (see Materials and Methods).

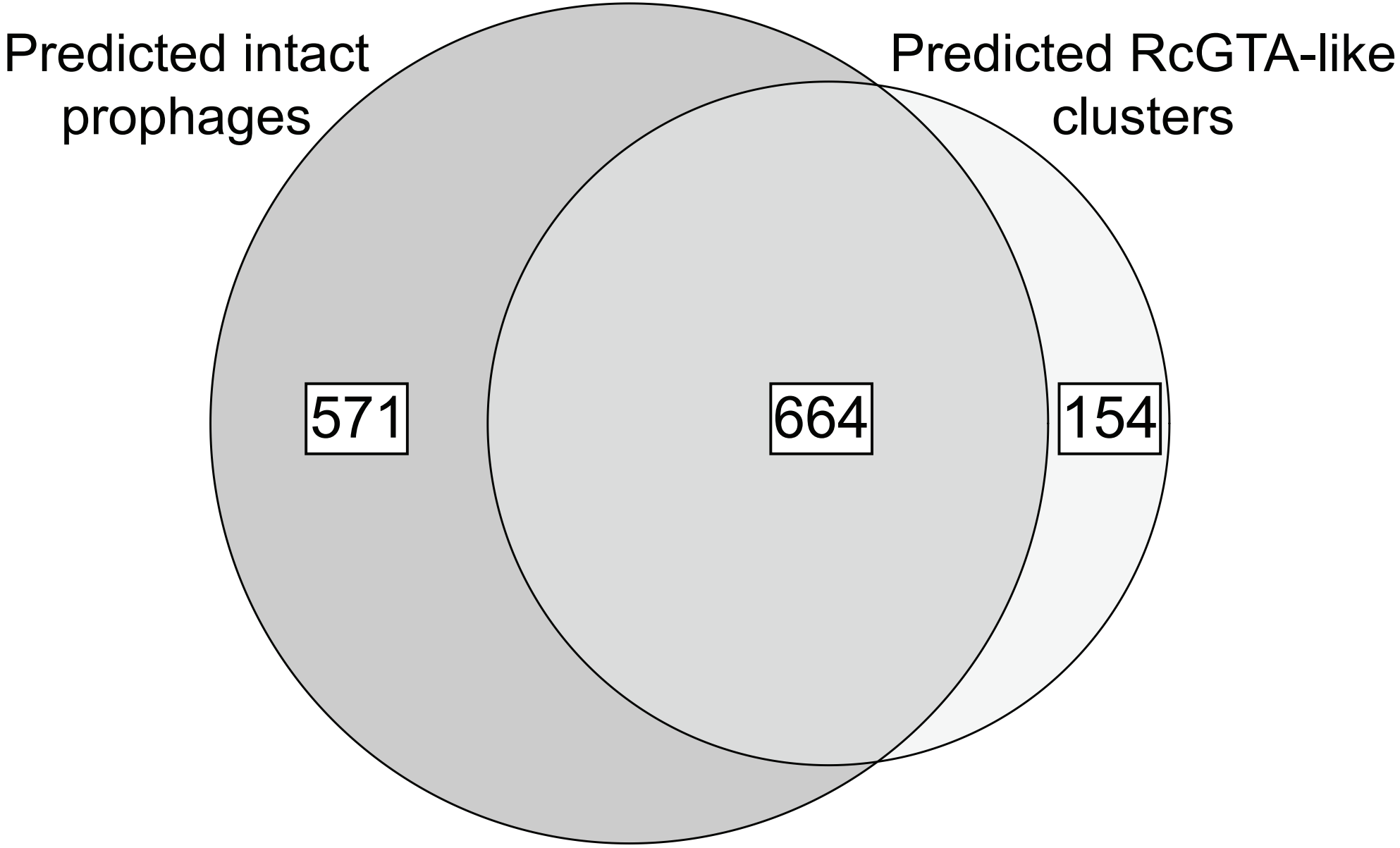

Figure 4. An overlap between prophage and GTA predictions. The “predicted RcGTA-like clusters” set refers to the GTA-Hunter predictions, while the “predicted intact prophages” set denotes predictions made by the PHASTER program (Arndt et al. 2016) on the subset of the genomes that are found within Clade 4 (Figure 3).

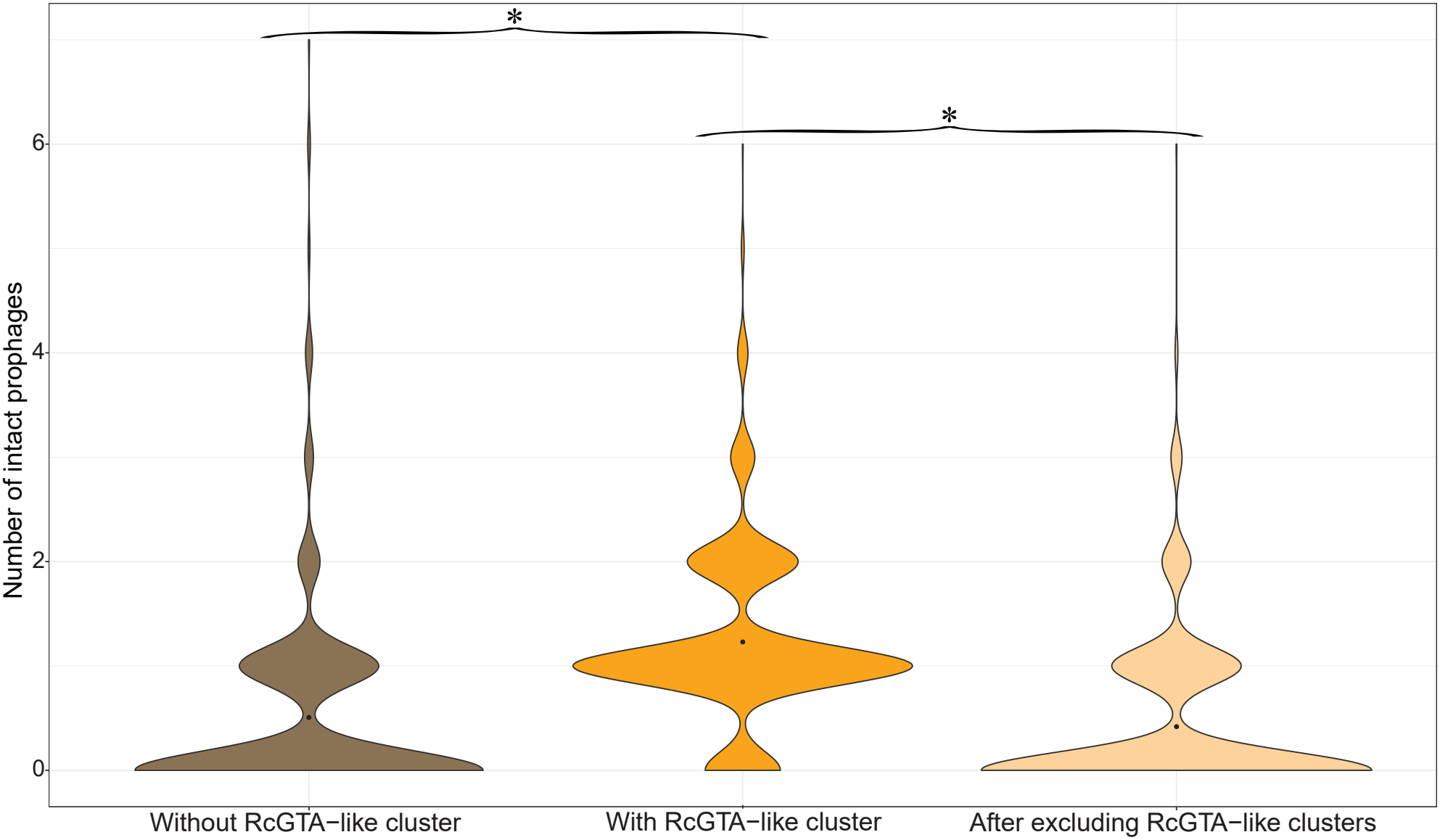

Figure 5. The number of predicted 'intact' prophages in alphaproteobacterial genomes. The 1,423 genomes were divided into two groups: those without GTA-Hunter-predicted RcGTA-like clusters (in brown) and those with these RcGTA-like clusters (in dark orange). For the latter group, the number of prophages was re-calculated after the RcGTA-like clusters that were designated as prophages were removed (in light orange). The distribution of the number of predicted intact prophages within each dataset is shown as a violin plot with the black point denoting the average value. The datasets with significantly different average values are denoted by asterisks ($p < 0.001$; Mann-Whitney U test).

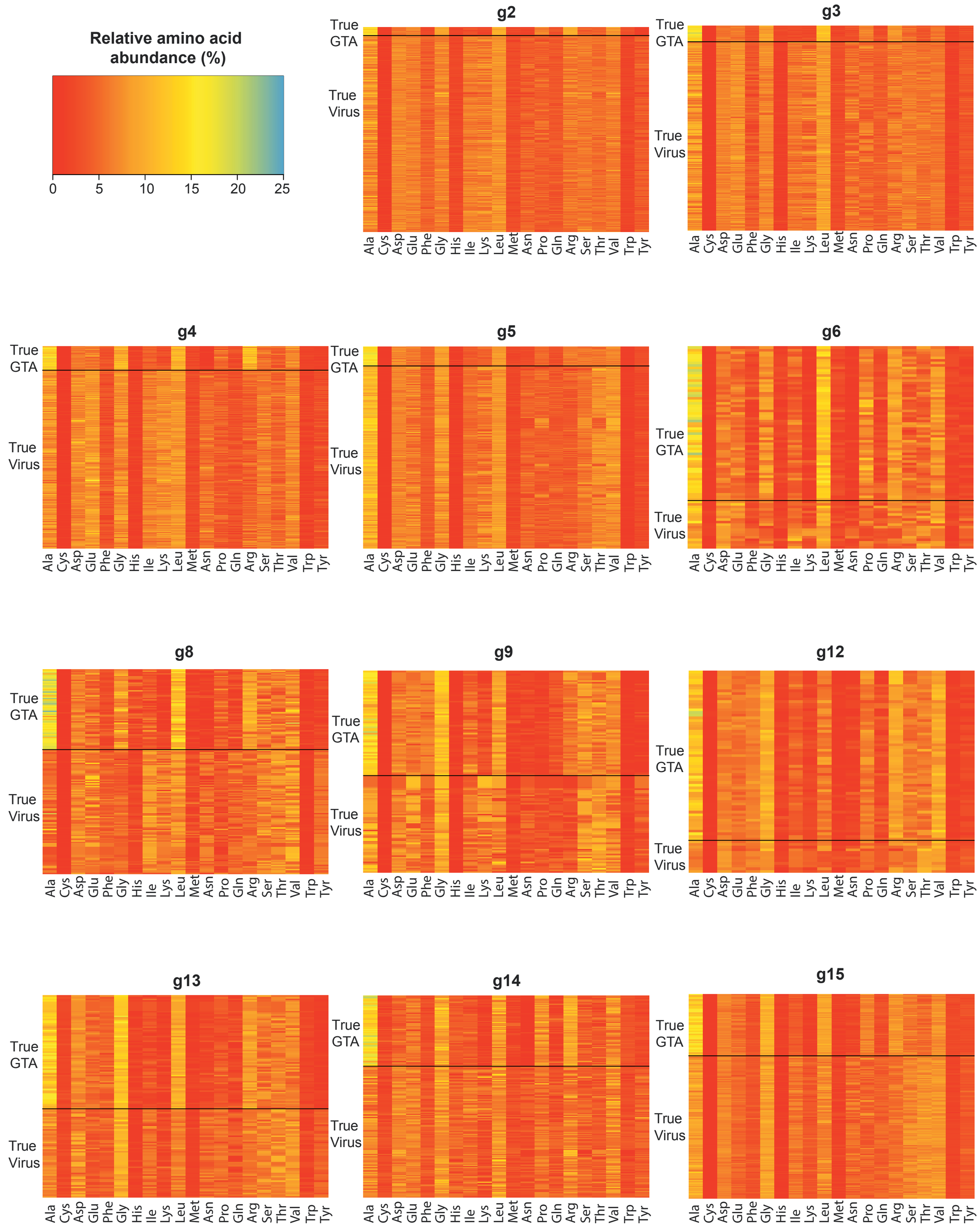

Supplementary Figure S1. The amino acid composition of viral and alphaproteobacterial homologs of the 11 RcGTA genes. These homologs were used in the training and cross-validation of the SVM classifier. Each heatmap corresponds to one of the 11 genes (see Supplementary Table S1 for the functional annotations of the genes). Each row in a heatmap corresponds to an individual homolog of the RcGTA gene. The homologs from viruses and alphaproteobacterial are separated by the black line and labeled as “True Virus” and “True GTA”, respectively. The heatmap shows the relative abundance of each amino acid within a homolog.

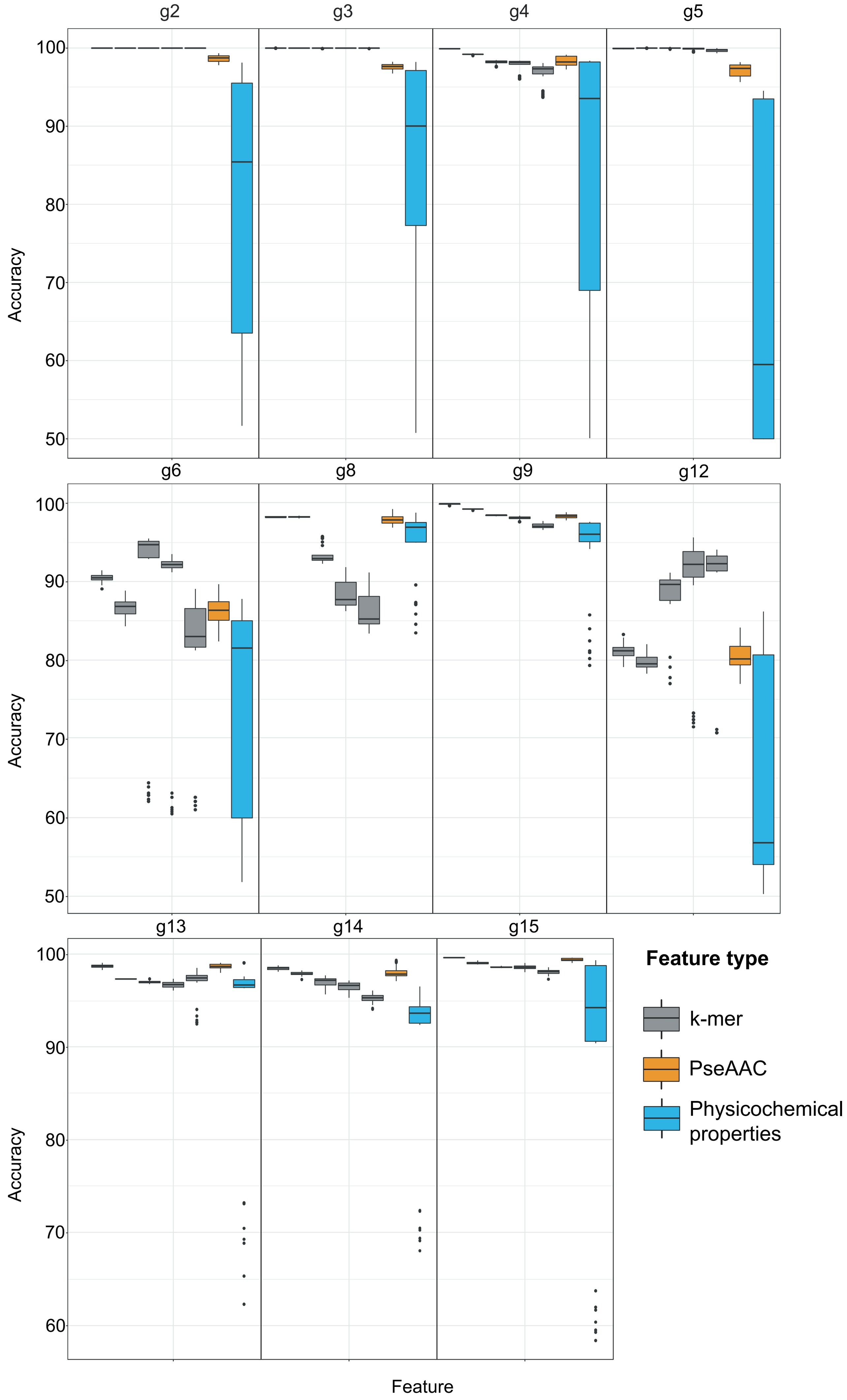

Supplementary Figure S2. The weighted accuracies for different types of features. The boxplots for the three feature types are color coded. The data for five examined k-mer sizes (2, 3, 4, 5, 6) are shown from the left to the right on the graphs. Each boxplot shows a median value bounded by the first and third quartiles, and the whiskers depict a deviation that was calculated using the 1.5*InterQuartile Range rule. Outliers are shown as dots.